Kinetic simulation of the non-equilibrium effects at the liquid-vapor interface

A.Ph. Polikarpov, Irina Graur, E.Ya. Gatapova, O.A. Kabov

₁ # Kinetic simulation of the non-equilibrium effects at the liquid-vapor interface

A. Ph. Polikarpov[1], I. A. Graur[2], E. Ya. Gatapova[3], O. A. Kabov[3]

[1]Ural Federal University, 51 str. Lenina, 620000 Ekaterinbourg, Russia
[2]Aix-Marseille Université, CNRS, IUSTI UMR 7343, 13013 Marseille, France
[3]Kutateladze Institute of Thermophysics SB RAS, Novosibirsk, 630090, Russia

Abstract

Phase change phenomena at microscale is important for novel cooling microsystems with intensive evaporation, so the development of reliable models and simulations are challenging. The vapor behaviors near its condensed phase are simulated using the non-linear S-model kinetic equation. The pressure and temperature jumps obtained numerically are in good agreement with the analytical expressions derived from the appropriate Onsager-Casimir reciprocity relations. The results of the evaporation flux are close to those given by the Hertz-Knudsen-Schrage formula, only when the values of the pressure and temperature at the upper boundary of the Knudsen layer are used. Comparison with recently measured temperature jumps are provided and disagreement with some experiments are discussed.

Keywords: liquid-vapor interface, evaporation rate, Knudsen layer, molecular mean free path, non-equilibrium state, temperature and pressure jumps

1. Introduction

Understanding of heat and mass transfer mechanisms at liquid-vapor interface is important not only from the fundamental point of view, but also for various applications, such as for the design and optimization of the cooling microsystems. During the evaporation process a thin layer, the Knudsen layer, forms near the liquid interface at the vapor side. Inside this layer, which thickness is of the order of several mean free paths, the vapor is in equilibrium state only when the flux of the evaporation molecules is equal to the flux of the condensed molecules. When a net evaporation (or condensation) flux exists a vapor near the interface is in non-equilibrium state and the continuity of the thermodynamic variables, like pressure and temperature, cannot be ensured anymore. This non-equilibrium behavior of a vapor cannot be described by the continuum equations and other approaches, as the gas kinetic theory and molecular dynamics have to be implemented.

From a two decades different authors [1], [2], [3], [4] have measured the liquid and vapor properties namely the temperature profiles and the temperature
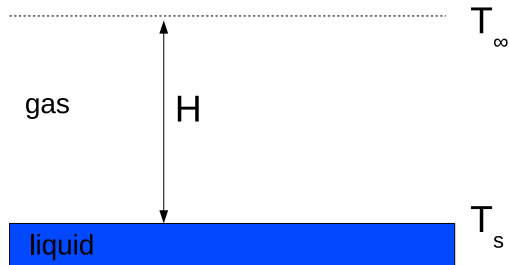
Figure 1: Problem configuration.

jump at the liquid-vapor interfaces. In all these experiments the temperature jump measured on the interface was found surprisingly large, much larger than that predicted by the kinetic theory of gases. Only recently, the new series of measurements [5], [6] have appeared, where the temperature jump was found of the same order as that predicted by the kinetic theory. However, still in recent papers [6], [7] the temperature in vapor near interface was measured higher compared to the interface temperature. The positive values of the temperature difference between liquid and vapor temperatures at interface (vapor temperature is lower than the interface temperature) were measured only by the authors of Ref. [5].

To go forward in the understanding of the flow behavior at liquid-vapor interface the gas flow evaporating from its condensed phase is investigated on the basis of the kinetic approach. The non-linear S-model kinetic equation [8] is solved numerically by the Discrete Velocity Method (DVM) [9]. The structure of the Knudsen layer is analyzed and the macroscopic temperature and pressure jumps, obtained from the numerical simulations, are compared with the analytical expressions derived by the authors of Ref. [10] from the kinetic theory of gases and the thermodynamics of irreversible processes. The experimental data of Refs. [4] and [6] are used as input parameters for the numerical analysis.

2. Problem statement

We consider a plane condensed phase at rest occupying the half space ($y' < 0$), and the gas (vapor) evaporating from this infinite planar surface kept at constant and uniform temperature T_s. The interface is located at $y' = 0$, where y' is the variable normal to the condensed phase surface, see Fig. 1. The steady one-dimensional flow is considered.

When a gas is near a surface (liquid or solid) a thin layer, the Knudsen layer, forms in the vicinity of the surface. The thickness of this layer is usually of the order of several molecular mean free paths. To estimate the thickness of this layer we use the equivalent mean free path defined as [11]:

$$\ell_s = \frac{\mu_s v_s}{p_s}, \tag{1}$$

using the reference parameters with subscript s, corresponding to the vapor characteristics at the condensed phase surface. In Eq. (1) $\mu_s = \mu(T_s)$ is the dynamic viscosity of the vapor phase

$$\mu(T') = \mu_s \sqrt{\frac{T'}{T_s}} \qquad (2)$$

at temperature T_s, v_s is the most probable molecular speed,

$$v(T') = \sqrt{2\mathcal{R}T'}, \qquad (3)$$

calculated also at the temperature T_s: $v_s = v(T_s)$, $\mathcal{R} = k_\mathrm{B}/m$ is the specific gas constant, k_B is the Boltzmann constant, m is the molecular mass.

The upper boundary of the computational domain is far from the evaporation surface, at the distance H, see Fig. 1. Different values of H are tested and finally $H = 25\ell_s$ is retained to do all the simulations.

3. S-model kinetic equation

To model the evaporation process of a monoatomic gas from its condensed phase the S-model kinetic equation [8] is used. The evaporation phenomenon is considered here as one dimensional in physical space, so the S-model kinetic equation is written as

$$\frac{\partial f}{\partial t'} + v_y \frac{\partial f}{\partial y'} = v'\left(f^S - f\right), \qquad (4)$$

where $f(t',y',\mathbf{v})$ is the one particle velocity distribution function, t' is the time, $\mathbf{v} = (\mathbf{v_x}, \mathbf{v_y}, \mathbf{v_z})$ is the molecular velocity vector, v' is the collision frequency, $v' = p'/\mu'$, p' is the gas pressure. In the frame of the S-model the equilibrium distribution function f^S in Eq. (4) is defined as following

$$f^S(t', y', \mathbf{v}) = f^M\left[1 + \frac{2m\mathbf{V}\mathbf{q}'}{15n'(y')(k_\mathrm{B}T'(y'))^2}\left(\frac{m\mathbf{V}^2}{2k_\mathrm{B}T'(y')} - \frac{5}{2}\right)\right], \qquad (5)$$

here $T'(y')$ is a gas temperature, $n'(y')$ is a gas number density, $\mathbf{u}' = (0, u'_y, 0)$ is a bulk velocity vector, $\mathbf{V} = \mathbf{v} - \mathbf{u}'$ is the peculiar velocity vector, $\mathbf{q}' = (0, q'_y, 0)$ is a heat flux vector, f^M is the Maxwellian distribution function [12]. The macroscopic parameters are defined as follows:

$$n'(y') = \int f(y', \mathbf{v})\mathrm{d}\mathbf{v}, \qquad u'_y(y') = \frac{1}{n'}\int f(y', \mathbf{v})v_y\mathrm{d}\mathbf{v},$$

$$T'(y') = \frac{m}{3k_\mathrm{B}n'}\int f(y', \mathbf{v})V^2\mathrm{d}\mathbf{v}, \quad q'_y(y') = \frac{m}{2}\int f(y', \mathbf{v})V^2(v_y - u'_y)\mathrm{d}\mathbf{v} \quad (6)$$

The evaporation flow rate, expressed in the number of molecules evaporating per seconds and per unit area, J'_n, and the evaporation mass flow rate, expressed

3

in mass of vapor (in kilogram) per second evaporating from a unit area, J'_m, are defined as following:

$$J'_n = \int v_y f(y', \mathbf{v}) \mathrm{d}\mathbf{v}, \qquad J'_m = m \int v_y f(y', \mathbf{v}) \mathrm{d}\mathbf{v}. \qquad (7)$$

The second definition of the evaporation mass flow rate is usually provided from the experiments. It is clear that previous relations represent the conservation of the number of particles and the mass conservation. Additionally, the y momentum and energy conservation are written as

$$J'_{v_y} = \int v_y^2 f(y', \mathbf{v}) \mathrm{d}\mathbf{v}, \qquad J'_E = m \int v_y v^2 f(y', \mathbf{v}) \mathrm{d}\mathbf{v}. \qquad (8)$$

The constancy of J'_m, J'_{v_y}, and J'_E will be used for the accuracy test of the applied numerical method.

4. Boundary conditions

The distribution function of evaporating molecules is assumed to be a half-range Maxwellian:

$$f(t, 0, \mathbf{v}) = (\sigma n_s + (1-\sigma)n_r) \left(\frac{m}{2\pi k_\mathrm{B} T_s} \right)^{3/2} \exp\left(-mv^2/(2k_\mathrm{B} T_s) \right), \quad v_y > 0, \tag{9}$$

were

$$n_r = -\sqrt{\frac{2\pi m}{k_\mathrm{B} T_s}} \int_{v_y < 0} f v_y \mathrm{d}\mathbf{v}. \tag{10}$$

Here n_s is the number density, calculated from the saturated surface temperature and pressure as $n_s = p_s/(k_\mathrm{B} T_s)$. The coefficient σ that is a part of the incident molecules evaporating immediately from the condensed surface, while $(1-\sigma)$ part of molecules is assumed to be reflected diffusively from the interface.

The uniform equilibrium vapor state (subscript ∞) is described by the equilibrium Maxwellian distribution function

$$f(t, H, \mathbf{v}) = \frac{p_\infty}{k_\mathrm{B} T_\infty} \left(\frac{m}{2\pi k_\mathrm{B} T_\infty} \right)^{3/2} \exp\left(-m(\mathbf{v} - \mathbf{u}_\infty)^2/(2k_\mathrm{B} T_\infty) \right), \quad v_y < 0, \tag{11}$$

where $\mathbf{u}_\infty = (0, u_{y\infty}, 0)$. As it was discussed in Refs. [13], [14], [15], in the case of evaporation, a solution of the boundary value problem exists only when some relations between the parameters are satisfied. In the case of evaporation these relations are given by [14]

$$\frac{p_\infty}{p_s} = h_1(Ma_{y\infty}), \qquad \frac{T_\infty}{T_s} = h_2(Ma_{y\infty}). \tag{12}$$

The functions h_1 and h_2 are obtained numerically and their tabulated values can be found in Ref. [14]. In the case of weak evaporation conditions, that means

4

104 that the variation from the uniform equilibrium state at reste with pressure and
105 temperature is small (or where the evaporation is weak, *i.e.* evaporation Mach
106 number is small compared to 1), the relations between three parameters become

$$\frac{p_\infty}{p_s} = 1 + C_4^* \frac{u_{y\infty}}{\sqrt{2\mathcal{R}T_s}}, \qquad \frac{T_\infty}{T_s} = 1 + d_4^* \frac{u_{y\infty}}{\sqrt{2\mathcal{R}T_s}}, \tag{13}$$

107 where $C_4^* = -2.13204$ and $d_4^* = -0.44675$, obtained with Boltzmann-Krook-
108 Welander (BKW) model in Ref. [16]. The previous relations give the boundary
109 conditions for the Euler equations. However, for the Navier-Stokes equations
110 more complet boundary conditions have to be used on the liquid-vapor interface,
111 which are discussed in Section 6.
112   The number and the nature of conditions (12) are different for evaporation
113 and condensation flows [14], [15].

114 5. Dimensionless form

115   For further derivation we introduce the following dimensionless quantities:

$$y = \frac{y'}{\ell_s}, \quad \mathbf{c} = \frac{\mathbf{v}}{v_s}, \quad \mathbf{u} = \frac{\mathbf{u}'}{v_s}, \quad t = t'\frac{v_s}{\ell_s}, \quad n = \frac{n'}{n_s}, \quad T = \frac{T'}{T_s}, \quad \mathbf{q} = \frac{\mathbf{q}'}{p_s v_s}. \tag{14}$$

116 Now the dimensionless S-model kinetic equation can be written in the form:

$$\frac{\partial f}{\partial t} + v_y \frac{\partial f}{\partial y} = n\sqrt{T} \left(f^S - f \right). \tag{15}$$

117 The dimensionless boundary conditions for the distribution function of the re-
118 flected molecules at the liquid-vapor interface can be written as

$$y = 0, \quad t > 0, \quad c_y > 0,$$

$$f(t, 0, \mathbf{c}) = (\sigma n_s + (1 - \sigma)n_r)f_s^M, \quad f_s^M = \frac{1}{\pi^{3/2}} \exp\left(-c^2\right). \tag{16}$$

119 The number density n_r can be calculated from the impermeability condition on
120 the condensed surface:

$$n_r = -2\sqrt{\pi} \int_{c_y < 0} c_y f \mathrm{d}\mathbf{c}. \tag{17}$$

121 As it was mentioned in previous section far from the condensed surface the gas is
122 supposed in equilibrium steady-state, so for the molecules coming from infinity
123 two parameters from three in the Maxwellian depend on the third one. Here we
124 fix the macroscopic flow velocity in the Maxwellian distribution function as

$$y = H, \quad t > 0, \quad c_y < 0, \qquad f_\infty^M = \frac{1}{\pi^{3/2}} \frac{p_\infty}{p_s} \left(\frac{T_s}{T_\infty}\right)^{5/2} \exp\left(-\frac{T_s}{T_\infty}(u_{y\infty} - c)^2\right). \tag{18}$$

125 At the upper boundary initially, at $t = 0$, all three parameters, p_∞, T_∞ and $u_{y\infty}$
126 are fixed, and the distribution function for the incoming molecules is calculated

127 from Eq. (18), then only the macroscopic velocity is still kept constant, but
128 other two parameters are obtained from previous time step.

129 To minimize the computational efforts, the c_z variable is eliminated by intro-
130 ducing the reduced distribution functions as in Ref. [17]. The Discrete Velocity
131 Method [9] was used to solve Eq. (15) with the boundary conditions Eqs. (16),
132 (17) and (18). The details of the numerical realization can be found in [18].

6. Jump boundary conditions

134 In this Section we present the jump boundary conditions by following the
135 approach based on the Onsager-Casimir reciprocity relations, as it was presented
136 in Ref. [19] for the case of evaporation and condensation of a gas between two
137 parallel condensed phases. In the case of evaporation from a plate liquid surface
138 we can introduce, by analogy with [19], the thermodynamic "forces" as following

$$X_P = \frac{p_\infty - p_s}{p_s}, \qquad X_T = \frac{T_\infty - T_s}{T_s}. \tag{19}$$

139 We assume then that the deviations between the temperature of the condensed
140 surface and that far from it and the corresponding pressures are small: $X_P \ll 1$
141 and $X_T \ll 1$. For a given gas the pressure and temperature differences are
142 coupled by the relation

$$p_s - p_\infty = \beta(T_s - T_\infty), \tag{20}$$

143 where β is a positive constant corresponding to the slop of the Clausius-Clapeyron
144 curve at T_s, so X_P and X_T are not independent quantities. However, here we
145 will consider two forces separately, to see clearly the impact of each force on the
146 evaporation process.

147 Following [19] we introduce the "fluxes" corresponding to the driving "forces"
148 as:

$$J'_P = -n_s u'_y, \qquad J'_T = -\frac{1}{k_{\mathrm{B}}T_s} q'_y, \tag{21}$$

149 where u'_y and q'_y do not depend on y. The thermodynamic fluxes are related to
150 the thermodynamic forces in the matrix form:

$$\begin{bmatrix} J'_P \\ J'_T \end{bmatrix} = \begin{bmatrix} \Lambda'_{PP} & \Lambda'_{PT} \\ \Lambda'_{TP} & \Lambda'_{TT} \end{bmatrix} \times \begin{bmatrix} X_P \\ X_T \end{bmatrix}. \tag{22}$$

151 The Onsager-Casimir relation $\Lambda'_{PT} = \Lambda'_{TP}$ in this case yields the coupling be-
152 tween the mass flux caused by temperature drop and the thermal flux caused
153 by the pressure drop [19].

154 Previous equation allows to express the thermodynamic fluxes in function of
155 the thermodynamic forces. In this way the expressions analogous to the Hertz-
156 Knudsen equation are obtained in the end of this Section. However, first we are

6

interested to express the thermodynamic forces in function of fluxes, so we can write

$$\begin{bmatrix} X_P \\ X_T \end{bmatrix} = \begin{bmatrix} \Lambda'_{PP} & \Lambda'_{PT} \\ \Lambda'_{TP} & \Lambda'_{TT} \end{bmatrix}^{-1} \times \begin{bmatrix} J'_P \\ J'_T \end{bmatrix} = \begin{bmatrix} a'_{11} & a'_{12} \\ a'_{21} & a'_{22} \end{bmatrix} \times \begin{bmatrix} J'_P \\ J'_T \end{bmatrix}. \qquad (23)$$

The elements $a'_{ij} = a_{ij}/(n_s v_s)$ in previous relation are obtained in [10], [20], from gas kinetic theory for the case of the diffuse reflection of the molecules from a surface. The coefficients a_{ij} have the following values:

$$a_{11} = 2\sqrt{\pi}\left(\frac{1}{\sigma} - b_{11}\right), \quad a_{12} = a_{21} = 2\sqrt{\pi}b_{12}, \quad a_{22} = 2\sqrt{\pi}b_{22}, \qquad (24)$$

where

$$b_{11} = \frac{1}{\pi} - \frac{23}{32}, \quad b_{12} = \frac{1}{16} + \frac{1}{5\pi}, \quad b_{22} = \frac{1}{8} + \frac{13}{25\pi}. \qquad (25)$$

The numerical values of a_{ij} coefficients for $\sigma = 1$ are the following

$$a_{11} = 2.125, \quad a_{12} = a_{21} = 0.447, \quad a_{22} = 1.030. \qquad (26)$$

In Ref. [10] a particular approximation method was used to evaluate the numerical values of a_{ij} coefficients. Other approximation methods have also been used and give slightly different values, see Ref. [14].

Finally the pressure and temperature jumps can be expressed as following:

$$\frac{p_s - p_\infty}{p_s} = a_{11}\frac{J'_m}{mn_s v_s} + a_{12}\frac{q'}{p_s v_s}, \qquad (27)$$

$$\frac{T_s - T_\infty}{T_s} = a_{21}\frac{J'_m}{mn_s v_s} + a_{22}\frac{q'}{p_s v_s}. \qquad (28)$$

In previous expressions J'_m and q' are the evaporation mass flux (7) and the heat flux (6) outside from the Knudsen layer in the continuum part of the flow. As it is clear from the previous relations that the intensity of pressure and temperature jumps is proportional to both mass and heat fluxes. It is worth to note that this form of jumps expression is similar to Eqs. (13), but in the present form the heat exchange is also considered.

As it was pointed out in [21] if one uses as the surface temperature the temperature of the adjacent liquid, the results found using non-equilibrium thermodynamics and the results obtained from the kinetic theory are in perfect agreement with each other.

We can also express the fluxes in the function of forces from Eq. (22) as

$$\begin{bmatrix} J'_P \\ J'_T \end{bmatrix} = \begin{bmatrix} \Lambda'_{PP} & \Lambda'_{PT} \\ \Lambda'_{TP} & \Lambda'_{TT} \end{bmatrix} \times \begin{bmatrix} X_P \\ X_T \end{bmatrix} = \begin{bmatrix} a''_{22} & -a''_{12} \\ -a''_{21} & a''_{11} \end{bmatrix} \times \begin{bmatrix} X_P \\ X_T \end{bmatrix}, \qquad (29)$$

where $a''_{ij} = a_{ij}n_s v_s/\mathcal{D}$ and $\mathcal{D} = a_{11}a_{22} - a_{12}a_{21}$. From (29) we have

$$\frac{J'_m}{mn_s v_s} = \frac{1}{\mathcal{D}}\left(a_{22}\frac{p_s - p_\infty}{p_s} - a_{12}\frac{T_s - T_\infty}{T_s}\right), \qquad (30)$$

$$\frac{q'}{p_s v_s} = \frac{1}{\mathcal{D}} \left(-a_{21} \frac{p_s - p_\infty}{p_s} + a_{11} \frac{T_s - T_\infty}{T_s} \right). \tag{31}$$

Previous relations are analogous to that obtained from non-equilibrium thermodynamics [21], [22]. We can provide the explicit expressions for the surface resistivities

$$\begin{aligned}
\frac{a_{22}}{\mathcal{D}} &= \frac{\sigma}{2\sqrt{\pi}(1 + \sigma(b_{11} - b_{12}^2/b_{22}))} = \frac{\sigma}{2\sqrt{\pi}(1 - 0.455\sigma)}, \\
\frac{a_{12}}{\mathcal{D}} &= \frac{\sigma b_{12}}{2\sqrt{\pi} b_{22}(1 + \sigma(b_{11} - b_{12}^2/b_{22}))} = \frac{0.434\sigma}{2\sqrt{\pi}(1 - 0.455\sigma)}, \\
\frac{a_{11}}{\mathcal{D}} &= \frac{1 + \sigma b_{11}}{2\sqrt{\pi} b_{22}(1 + \sigma(b_{11} - b_{12}^2/b_{22}))} = \frac{1 - 0.4\sigma}{2\sqrt{\pi} 0.291(1 - 0.455\sigma)}.
\end{aligned} \tag{32}$$

The numerical values of the coefficients provided above for evaporation coefficient equal to 1 are:

$$\frac{a_{22}}{\mathcal{D}} = 0.517, \qquad \frac{a_{12}}{\mathcal{D}} = 0.225, \qquad \frac{a_{11}}{\mathcal{D}} = 1.068. \tag{33}$$

6.1. Hertz-Knudsen-Schrage formula

More than one hundred year ego Hertz and Knudsen [23], considering only the fluxes balance near the liquid interface, proposed the equation which relate the evaporation flux to the liquid temperature (and pressure) and to the parameters on the upper boundary of the Knudsen layer. The flux of the particles evaporated from a surface was estimated from the gas kinetic theory as

$$J'_n = \frac{n_s v_{ms}}{4}, \qquad \text{where} \qquad v_{ms} = \sqrt{\frac{8k_{\mathrm{B}} T_s}{\pi m}}, \tag{34}$$

where v_{ms} is the average molecular velocity at the interface temperature. The same molecular flux comes to the interface from the Knudsen layer with the parameters n_∞ and T_∞. The balance of the fluxes allows to derive the Hertz-Knudsen formula

$$J'_m = \sqrt{\frac{m}{2\pi k_{\mathrm{B}}}} \left(\frac{p_s}{\sqrt{T_s}} - \frac{p_\infty}{\sqrt{T_\infty}} \right). \tag{35}$$

This expression was improved by Kucherov and Rikenglas [24], [25] and then by Schrage [26] by taking into account the macroscopic vapor velocity and by introducing the evaporation coefficient as:

$$J'_m = \frac{2\sigma}{2 - \sigma} \sqrt{\frac{m}{2\pi k_{\mathrm{B}}}} \left(\frac{p_s}{\sqrt{T_s}} - \frac{p_\infty}{\sqrt{T_\infty}} \right). \tag{36}$$

Later, many various modifications of this expression were proposed to much it with the measurements. However, this formula provides the evaporation flux

much larger that one found in experiments [4] for measured large value of the temperature jump. We show in the next Section that this expression works well only when the p_∞ and T_∞ are taken in the upper boundary of the Knudsen layer, where it is very difficult to make the measurements because of the very thin thickness of this layer.

6.2. Comments on Jumps

It is worth to discuss first the definition of the temperature jump as it is used in the kinetic theory. This jump is defined as a difference between the solid (or liquid) surface temperature, T_s, and the gas temperature near the surface, $T|_{y=0}$. It is well known [27], [14] that the near a surface a very thin layer, the Knudsen layer, exists, which thickness is of the order of several molecular mean free path. Inside this layer the continuum approach does not valid any more. Therefore the temperature jump boundary condition is used for the Navier-Stokes (NS) equations:

$$T|_{y=0} - T_s = \xi_T \ell \frac{dT}{dy}, \tag{37}$$

where ξ_T is the temperature jump coefficient [12], [11]. This condition assures that the solution of the NS equation with the jump condition coincide with the solution of the Boltzmann equation (or of other kinetic equations) on the upper boundary of the Knudsen layer. It is clear from Eq. (37) that in the case of the gas - solid interface the temperature jump $(T|_{y=0} - T_s)$ is proportional to the molecular mean free path. Therefore this jump becomes negligible under atmospheric conditions where the molecular mean free path is small, of the order of a micron. This temperature jump has to be taken into account either under reduced pressure conditions or in the microsystem applications, when the characteristic length-scale of a flow is of order of tens hundred microns.

When the liquid–gas interface is considered, this difference between the gas temperature and surface temperature, $T_s - T|_{y=0}$, exists also. However, historically, the difference between the temperature at the upper boundary of the Knudsen layer and the surface temperature, $T_s - T|_{y=H}$ is called the temperature jump. As in the case of the gas-solid interface the NS equations do not valid inside the Knudsen layer. Therefore, the boundary conditions, Eqs. (27), (28), are proposed to use for the Navier-Stokes equations [28] to take into account the Knudsen layer influence. The implementation of these conditions ensure that both solutions: the solution of the NS equations with temperature and pressure jump boundary conditions and the solution of the kinetic equation coincide on the upper boundary of the Knudsen layer.

In addition, contrarily to the gas-solid interface, in the case of the gas-liquid interface one more condition for the pressure jump exists. Both pressure and temperature jumps are proportional to the mass and heat fluxes, and so depend on their intensity.

Figure 2 schematically demonstrates the temperature profile normal to the liquid-vapor interface, located at $y = 0$, as it can be obtained from the solution of a kinetic equation, see also next Section with the numerical results. From

9
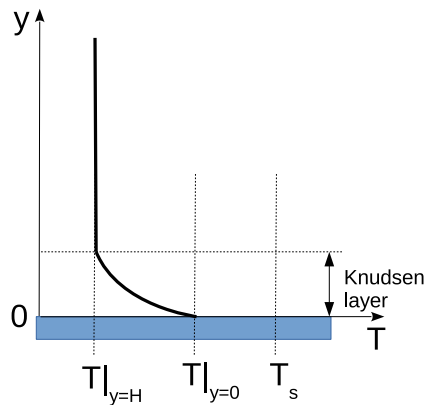
Figure 2: Temperature profile and temperature jump definition at liquid-vapor interface.

Fig. 2 it is clear that the strong temperature gradient is observed inside the Knudsen layer, then the temperature reaches asymptotically its value far from the Knudsen layer in the continuum region. In adopted here simulations we assume the absence of the macroscopic parameter gradient outside of the Knudsen layer.

7. Results

We present here a first step of application of non-linear S-model kinetic equation for modeling of evaporation process in the case, where the calculations have been made under assumption of the constant temperature in the vapor continuum region, so the heat flux in vapor phase is negligible. However, the model can be adopted to the situation, when the heat flux is important in the vapor continuum region.

7.1. Comparison with experiments

Recently several experiments are carried out to measure the temperature discontinuities on the liquid-gas interfaces in the case of pure substance evaporation [3], [4], [6] and in the case of presence of non-condensable gas [5]. We analyse here the experimental results, provided from Refs. [4] and [6], where evaporation process of pure substance (water) is considered. To compare with the measurements of the water evaporation the expressions provided in [29] is used to calculate the saturation pressure value from the measured liquid water

	Operating conditions [4]		
experimental data	$30°C$	$50°C$	$80°C$
$T_s(°C)$	2.65	4.66	-9.76
$p_s(Pa)^1$	738.8	851.2	291.9
$T_v(°C)$	6.64	10.91	4.69
$p_v(Pa)$	736.0	847.9	288.1
$J \times 10^4[kg/(m^2s)]$	5.78	7.66	11.9
$q \times 10^4[W/m^2]$	-231.45	-396.63	-650.56

Table 1: Experimental data from Ref. [4]. The saturation pressure $p_s{}^1$ is calculated from the saturation temperature by using the expression provided in Ref. [29].

temperature:

$$p_{sat}(T) = k_1 \exp(k_2 - k_3/T + k_4T - k_5T^2 + k_6T^3 - k_7T^4 - k_8 \ln(T)),$$
$$k_1 = 611.2 \quad k_2 = 1045.8511577 \quad k_3 = 21394.6662629 \quad k_4 = 1.0969044$$
$$k_5 = 1.3003741 \times 10^{-3} \quad k_6 = 7.747298 \times 10^{-7} \quad k_7 = 2.1649005 \times 10^{-12}$$
$$k_8 = 211.3896559. \tag{38}$$

It is worth to underline that the specific temperature range of the liquid water was used in the experiments, namely, the water was maintained at the liquid state for the temperatures below $0°C$, *i.e.* below its triple point. As it was mentioned in [29], the water is metastable in this temperature range and the measurements are impacted by the possibility of ice formation.

The S-model allows us to calculate the evaporation properties of the monoatomic gas. However, the numerical results are compared with the experiments made with water evaporation. To do this, first, all the numerical results were obtained in dimensionless form, then, to provide the dimensional values of the parameters of interest the water vapor properties are implemented. In addition, it was shown in Refs. [30], [15], that for the small evaporation rate the influence of the internal degree of freedom of a molecule on the temperature and pressure jumps is still negligible, which justifies here the implementation of the monoatomic gas model.

Three sets of experimental data from Ref. [4] and three sets from Ref. [6] were used as initial conditions for the numerical calculations and all these data are provided in Tables 1 and 2. The indications $30°C$, $50°C$ and $80°C$ are used to refer to the operating conditions from Ref. [4]. All simulations have been made with the evaporation coefficient equal to 1.

Figures 3 (a)-(d) show the profiles of the pressure in [Pa] and temperature [∘C] as a function of a distance (in [μm]) from the liquid surface for two cases, heating $30°C$ and $50°C$, from the experimental data of Ref. [4]. For each Figure the maximum value on the y axis corresponds to the value of saturation pressure (temperature) of the liquid layer. Both temperature and pressure jumps are visible on Figures and they are associated to the difference between the saturated values on the interface and on the upper boundary of the Knudsen layer.

11

experimental data	Operating conditions [6]		
	case 1	case 4	case 7
$T_s(^{\circ}C)$	-10.82 ± 0.05	-4.52 ± 0.05	4.08 ± 0.05
$p_s(Pa)$	265.7 ± 1.3	435.7 ± 2.2	815.5 ± 4.1
$p_s(Pa)^1$	268.43	437.17	817.28
$J \times 10^4 [kg/(m^2 s)]$	3.6350	3.1967	1.9532

Table 2: Experimental data from Ref. [6]. The saturation pressure $p_s{}^1$ is calculated from the saturation temperature by using the expression provided in Ref. [29]. The values of the evaporation flux were additionally provided by the authors of Ref. [6].

For two surface temperatures, $T_s = 2.65^{\circ}$C and $T_s = 4.66^{\circ}$C and corresponding saturation pressures, see Table 1, the molecular mean free path, estimated using Eq. (1), is equal to 6.31 μm and 5.60 μm, respectively, so the Knudsen layer thickness for both cases is of the order of 2 mean free paths. It is worth to note that here we use the so-called equivalent mean free path, Eq. (1), while various other definitions exist in the literature, which take into account different molecular interaction models. However, all these expressions provide similar order of magnitude of the mean free path. We would like also to underline that the calculated numerically Knudsen layer thickness is much smaller than thermocouple bed size, used in experiments [4], which was referred to be of 25 μm.

The profiles of the heat flux, in $[W/m^2]$, are also presented on Fig. 3 (e) and (f). The heat flux changes its sign through the Knudsen layer: it is positive near the liquid surface and become negative outside of this layer.

From Figure 3 it is clear that all parameters have the gradients inside the Knudsen layer, which thickness is around of 10 μm for two cases. Outside the Knudsen layer all parameters are quasi constant. It is worth to note that only one dimensional problem is considered here, therefore the constancy of the mass, momentum and full energy fluxes have to be conserved. However, the numerical values of the mass, momentum and full energy fluxes, Eqs. (7) and (8), which should theoretically be constant, show small variations over $0 < y < 1$. To quantify these variations we introduce the deviation, $\mathrm{dev}(J)$, of the numerical values of a flux from its average, [31] *i.e.*,

$$\mathrm{dev}(J) = \frac{1}{N_y} \sum_{j=1}^{N_y} \frac{|J(y_j) - J_{av}|}{|J_{av}|}, \qquad J_{av} = \frac{1}{N_y} \sum_{j=1}^{N_y} J(y_j), \qquad (39)$$

here N_y is the number of the computational points between 0 and 1 in y direction. These deviations for the evaporation (mass) and energy fluxes are provided in Table 3 and they are used as the accuracy test of the numerical computations.

As it is clear from Figure 3 the gradients of all macroscopic parameters exist in the Knudsen layer. As the continuum approach does not allow to simulate the flow behaviors inside the Knudsen layer the values obtained from the numerical solution of the S-model kinetic equation, *i.e.* the value on the upper boundary of the Knudsen layer, must be used as the boundary conditions,

Operating conditions [4]	$\mathrm{dev}(J_m) \times 10^{-5}$	$\mathrm{dev}(J_E) \times 10^{-5}$
$30^{\circ}C$	0.203	0.170
$50^{\circ}C$	0.237	0.171
$80^{\circ}C$	0.303	0.179

Table 3: Deviations, Eq. (39) for the evaporation (mass) and full energy fluxes for different experimental conditions from Ref. [4].

Operating conditions [4]	$J'_m \times 10^4 \ [kg/(m^2 s)]$				
	Eq. (30)	HKS[1]	HKS[2]	S-model	[4]
$30^{\circ}C$	5.17	179.8	5.49	5.88	5.78
$50^{\circ}C$	8.73	281.7	9.39	7.86	7.66
$80^{\circ}C$	12.80	261.1	13.74	12.70	11.9

Table 4: Mass flow rate $J'_m \times 10^4$ in $kg/(m^2 s)$, obtained from: Eq. (30), second column; HKS[1], Hertz-Knudsen-Schrage formula (36) with experiment data T_s (p_s) and $T_\infty = T_v$, $p_\infty = p_v$ from [4], third column; HKS[2], Hertz-Knudsen-Schrage formula (36) with experimental data T_s (p_s), T_∞ and p_∞ are taken from numerical solution of the S-model kinetic equation, fourth column; numerical S-model results, fifth column; experimental data [4], sixth column.

when the continuum approach is applied with the Navier-Stokes equation in order to describe correctly the interface behaviors.

Table 4 gives the values of the average over distance evaporation rate J'_m, obtained by different ways. Second column presents the results derived from the Onsager-Casimir theory, Eq. (30), with the pressure and temperature values, p_∞ and T_∞, obtained numerically from the solution of the S-model kinetic equation; third column, HKS[1], Hertz-Knudsen-Schrage formula (36) with experiment data [4], with T_s (p_s) and $T_\infty = T_v$, $p_\infty = p_v$ given in Table 1; fourth column HKS[2], Hertz-Knudsen-Schrage formula (36) with T_∞ and p_∞ obtained from numerical solution of the S-model kinetic equation; fifth column presents the numerical S-model results, sixth column contains the experimental data [4].

Analyzing the results presented in Table 4 we can conclude that the numerical solution of the S-model kinetic equation provides the results on the evaporation mass flow rate which are very close to the measured values. In addition, expression (30), obtained from Onsager-Casimir theory gives also very similar values of the evaporation flow rate, when the values p_∞ and T_∞ are taken from the numerical results. The Hertz-Knudsen-Schrage expression for mass flow rate, Eq. (36), calculated also with the numerical S-model results gives also similar values. However, when the same Hertz-Knudsen-Schrage expression, Eq. (36), is used but with $p_\infty = p_v$ and $T_\infty = T_v$ (see Table 1) much larger values for the evaporation mass flow rate is obtained. It means that the temperature T_v and pressure p_v, measured in Ref. [4], do not correspond to the upper boundary of a Knudsen layer. Therefore, Eq. (36) overestimates the evaporation rate, when temperature and pressure of vapor are taken at some distance outside the Knudsen layer.

One additional comment related to the extraction of the evaporation coeffi-

Operating conditions [4]	$T_s - T_\infty$ $[^\circ C]$			
	[4]	Eq. (28)[1]	Eq. (28)[2]	S-model
$30^\circ C$	-3.99	-0.15	0.025	0.036
$50^\circ C$	-6.25	-0.23	0.029	0.028
$80^\circ C$	-14.44	-1.09	0.131	0.124

Table 5: Temperature jump $T_s - T_\infty$ in $^\circ C$, obtained from: experiments [4], second column; Eq. (28)[1], with experimental values of J'_m and q' from [4], third column; Eq. (28)[2], where numerical values of J'_m and q' from numerical solution using S-model equation are used, fourth column; numerical S-model results, fifth column.

cient can be done. Usually, to extract the values of this coefficient, the Hertz-Knudsen-Schrage expression for evaporation rate, Eq. (36), is implemented. But usually the experimental values of the vapor temperature and pressure far from the liquid interface are used. Therefore, in order to much the measured evaporation rate given by Eq. (36) very small evaporation coefficient have to be used. In our opinion the large amount of the experimental data on the evaporation coefficient, where its value was found very small, can be related to this error.

The values of the temperature jump, *i.e.* the difference between the interface temperature, T_s, and the vapor temperature at the upper boundary of the Knudsen layer, T_∞, are given in Table 5. Second column provides the measured values of this jump; third column gives the values, calculated from Onsager-Casemir relation, Eq. (28), but using the measured in [4] evaporation rate and heat flux; forth column presents the value obtained from the same Onsager-Casemir relation, Eq. (28), but with evaporation rate and heat flux, obtained numerically from the solution of the S-model kinetic equation; forth column gives the temperature jump obtained numerically. One can see that the experimental values are very large compared to the values obtained numerically for very similar evaporation rate.

Table 6 provides the values of the temperature jump obtained for three sets of the experimental conditions from Ref. [6] (see also Table 2). As for the experimental data from Ref. [4] the calculated temperature jump is notably smaller than the measured one, despite the fact that the evaporation flux is reproduced numerically with very good accuracy, see Table 7. In addition, for two experimental data Refs. [4] and [6], the calculated vapor temperature near the liquid interface is found lower than that measured one. This fact could be partially explained by the formulation of the boundary condition on the upper boundary of the Knudsen layer. In both experiments the negative (directed to the liquid interface) heat flux exists in the vapor phase outside the Knudsen layer, while in the present form of the boundary condition at the upper boundary of the Knudsen layer the constant vapor temperature is assumed.

The values of the pressure jump, *i.e.* $p_s - p_\infty$ are provided in Table 8. Second column gives the jump values calculated from Eq. (27) using numerical values of the evaporation rate and heat flux; third column provides the values obtained directly from the numerical solution of the S-model kinetic equation. The values

	$T_s - T_\infty \ [^\circ C]$	
Operating conditions [6]	[6]	S-model
case 1	-0.36	0.039
case 4	-0.24	0.022
case 7	-0.14	0.0075

Table 6: Temperature jump, $T_s - T_\infty$, in $[^\circ C]$, comparison with the measured values from Ref. [6].

	$J'_m \times 10^4 \ [kg/(m^2 s)]$	
Operating conditions [6]	[6]	S-model
case 1	3.6350	3.6329
case 4	3.1967	3.1957
case 7	1.9532	1.9530

Table 7: Evaporation flux J'_m in $[kg/(m^2 s)]$, comparison with measured values from Ref. [6].

of the pressure jump obtained from both approaches are very similar.

Finally, the validation and improvement of the presented kinetic approache should be done by the detailed comparison with the precise measurements for different operating conditions requiring different rarefaction regimes. Such experimental data are practically missing. Such kind of data can be obtained by the contact methods which use the microthermocouples as well as by the more difficult in the realization non-contact methods. As it was pointed out above, the pressure and temperature discontinuities on the vapor-liquid interface are proportional to the evaporation rate and the heat flux through the interface. Therefore, for the future experiments this point should be taken into account to develop a new measurement system.

8. Conclusions

The kinetic approach is developed for numerical simulation of the evaporation process from a liquid surface. This approach allows the detailed simulations of the vapor flow behaviors above its condensed phase. The temperature jumps obtained numerically for different experimental conditions were found of the

	$p_s - p_\infty [Pa]$	
Operating conditions [4]	Eq. (27)	S-model
$30^\circ C$	0.32	0.29
$50^\circ C$	0.43	0.46
$80^\circ C$	0.69	0.67

Table 8: Pressure jump $p_s - p_\infty$ in $[Pa]$, obtained from: Eq. (27), where numerical values of J'_m and q' from numerical solution using S-model equation are used, second column; numerical S-model results, third column.

same order as that measured recently and presented in Refs. [6], [5], but much smaller than that found previously in Ref. [4]. The comparison with the experimental data from Ref. [4] shows that the vapor parameters are measured in [4] very far from the upper boundary of the Knudsen layer and therefore the application of the Knudsen-Hertz-Schrage formula predicts much higher mass flow rate as it was really measured. In addition, if the values of the pressure and temperature at the upper boundary of the Knudsen layer, obtained from the numerical solution of the S-model kinetic equation, are implemented in the Knudsen-Hertz-Schrage formula the evaporation rate is in excellent agreement with the measured one. The proposed approach could be used for the measurements of the evaporation coefficient.

In addition, the measured and calculated evaporation fluxes are very close each other. However, the calculated vapor temperature is found to be lower than that of the liquid interface, while in the analyzed experiments [4], [6] the measured near the liquid surface vapor temperature is higher than that of the liquid phase. This fact could be partially explained by the assumption of the constant vapor temperature made in the numerical simulations. To improve the simulations the boundary conditions could be modified to take into account the presence the heat flux in the vapor phase. In addition, to account more precisely the heat and mass exchanges between two phases the coupling between the continuum and kinetic approaches could be also realized.

In practice very often the evaporation of one substance in the presence of a non-condensable takes place, as in many cooling devices. Therefore, the next step will be the simulation of the fluid evaporation into a mixture of the evaporated fluid and non-condensable gas by using the kinetic approach. The numerical results will be compared to the available experimental data [5].

9. Acknowledgements

[1] P. N. Shankar and M. D. Deshpande. On the temperature distribution in liquid–vapor phase change between plane liquid surfaces. Physics of Fluids A., 2:1030–1038, 1990.

[2] C. A. Ward and G. Fang. Expression for predicting liquid evaporation flux: Statistical rate theory approach. Phys. Rev. E, 59:429–440, Jan 1999.

[3] C. A. Ward and D. Stanga. Interfacial conditions during evaporation or condensation of water. Phys. Rev. E, 64:051509, Oct 2001.

[4] V K Badam, V Kumar, F Durst, and K Danov. Experimental and theoretical invesigations on interfacial temerature jumps during evaporation. Experimental Thermal and Fluid Science, 32:276–292, 2007.

[5] E Ya Gatapova, I Graur, O A Kabov, V A Aniskin, M A Filipenko, and F Sharipov. The temperature jump at water-air interface during evaporation. Int. J. Heat Mass Transfer, 2017.

[6] M A Kazemi, D S Nobes, and J AW Elliott. Experimental and numerical study of the evaporation of water at low pressures. Langmuir, 33(18):4578–4591, 2017.

[7] P Jafari, A Masoudi, P Irajizad, M Nazari, V Kashyap, B Eslami, and H Ghasemi. Evaporation mass flux: A predictive model and experiments. Langmuir, 34:11676–11684, 2018.

[8] E M Shakhov. Generalization of the Krook kinetic relaxation equation. Fluid Dyn., 3(5):95–96, 1968.

[9] J E Broadwell. Shock structure in a simple discrete velocity gas. Physics of fluids, 7(8):1243–1247, 1964.

[10] J W Cipolla Jr, H Lang, and S K Loyalka. Kinetic theory of condensation and evaporation. II. J. Chem. Phys., 61:69–77, 1974.

[11] F Sharipov. Rarefied Gas Dynamics. Fundamentals for Research and Practice. Wiley-VCH, Berlin, 2016.

[12] M N Kogan. Rarefied gas dynamics. Plenum Press New York, 1969.

[13] Y Sone and H Sugimoto. Strong evaporation from a plane condensed phase. In Adiabatic waves in liquid-vapor systems, pages 293–304. Springer, New York, 1990.

[14] Y Sone. Kinetic Theory and Fluid Mechanics. Birkhäuser, Boston, 2002.

[15] A Frezzotti. Bondary conditions at vapor-liquid interface. Physics of Fluids, 23:030609, 2011.

[16] Y Sone and Y. Onishi. Kinetic theory of evaporation and condensation - hydrodynamic equation and slip boundary condition. J. Phys. Soc. Japan, 44:1981–1994, 1978.

[17] I A Graur and A Polikarpov. Comparison of different kinetic models for the heat transfer problem. Heat and Mass Transfer, 46:237–244, 2009.

[18] M T Ho, L Wu, I Graur, Y Zhang, and Reese J M. Comparative study of the Boltzmann and McCormack equations for Couette and Fourier flows of binary gaseous mixtures. Int. J. Heat Mass Transfer, 96:29–41, 2016.

17

[19] F Sharipov. Onsager-casimir reciprocity relations for open gaseous systems at arbitrary rarefaction. II Application of the theory for single gas. Physica A, 203:457–485, 1994.

[20] H. Lang. Evaporation and condensation for general gas-liquid surface scattering. J. Chem. Phys., 62(3):858–863, 1975.

[21] D Bedeaux, L J F Hermans, and T Ytrehus. Slow evaporation and condensation. Physica A, 169:263–280, 1990.

[22] D Bedeaux and S Kjelstrup. Transfer coefficients for evaporation. Physica A, 270:413–426, 1999.

[23] M Knudsen. Die maximale verdampfungsgeschwindigkeit des que-cksilbers. Ann. Phys. Chem., 47:697–708, 1915.

[24] R Y Kucherov and L E Rikenglas. Slipping and temperature discontinuity at the boundary of a gas mixture. Zh. Eksp. Teor. Fiz., 36(6):125, 1959.

[25] R Y Kucherov and L E Rikenglas. On hydrodynamic boundary conditions for evaporation and condebsation. Sov. Phys. JETP, 10(37):88–89, 1960.

[26] A Schrage. A Theoretical Study of Interphase Mass Transfer. Columbia University Press, New York, 1953.

[27] C Cercignani. Theory and application of the Boltzmann equation. Scottish Academic Press, Edinburgh, 1975.

[28] E Ya Gatapova, I Graur, F Sharipov, and O A Kabov. The temperature and pressure jumps at the vapor-liquid interface: Application to a two-phase cooling system. Int. J. Heat Mass Transfer, 83:235–243, 2015.

[29] F Duan, I Thompson, and C A Ward. Statistical rate theory determination of water properties below the triple point. J. Chem. Phys., 112:8605–8613, 2008.

[30] A Frezzotti. A numerical investigation of the steady evaporation of a polyatomic gas. European Journal of Mechanics Series B Fluids, 26(1):93–104, 2007.

[31] K Aoki and N Masukawa. Gas flows caused by evaporation and condensation on two parallel condensed phases and the negative temperature gradient: numerical analysis by using a nonlinear kinetic equation. Phys. Fluids, 6(3):1379–1395, 1994.
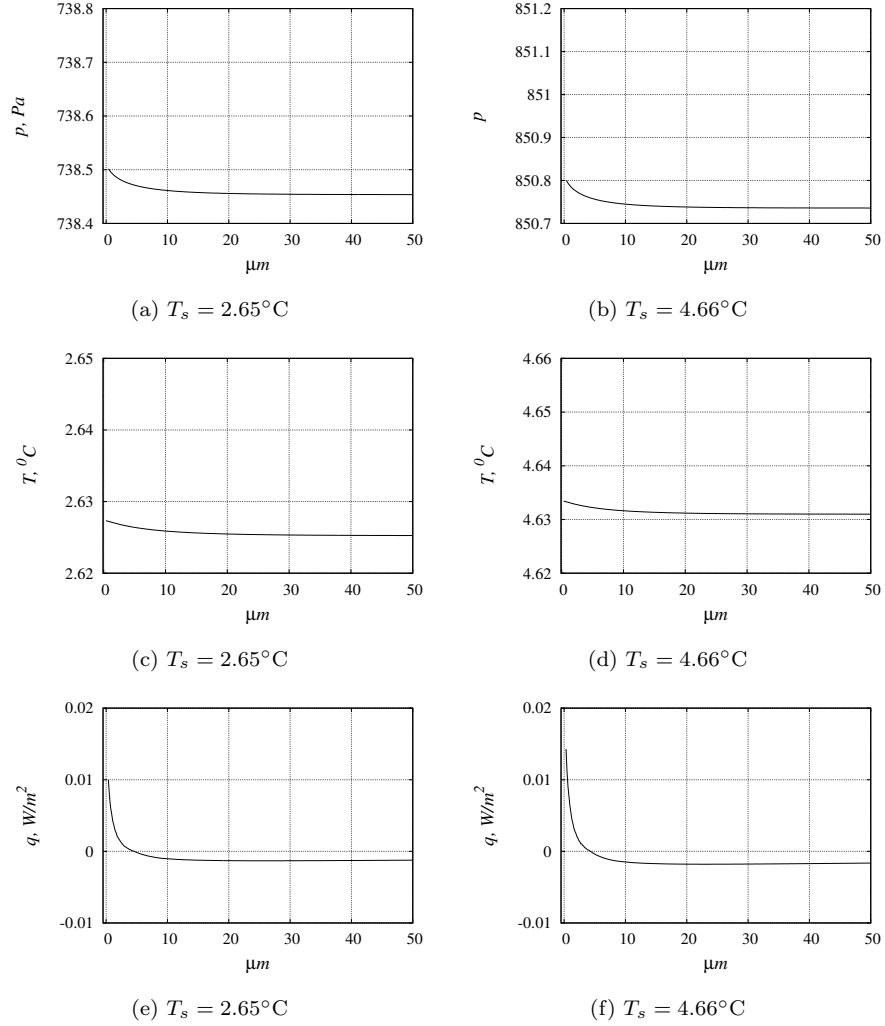
Figure 3: (a) and (b) pressure profiles, (c) and (d) temperature profiles, (e) and (f) heat flux profiles. All the profiles are obtained numerically using the experimental data [4], provided in Table 1, which correspond to heating $30°C$ and $50°C$, for (a),(c),(e) and (b),(d),(f), respectively. For figures (a)-(d) the maximal value on y axis corresponds to the saturation pressure (a),(b) and temperature (c),(d) of the interface.